OLEDs

DOI: 10.1002/anie.200805969

Photoprogrammable Organic Light-Emitting Diodes

*Philipp Zacharias, Malte C. Gather, Anne Köhnen, Nina Rehmann, and Klaus Meerholz**

Photochromism is generally known as the photoinduced change between two isomers with different absorption spectra. Well-established classes of photochromic dyes include anthracenes, spiropyrans, spirooxazines, chromenes, fulgides, azo compounds, and diarylethenes.[1] In most cases, thermal relaxation occurs, and the photostationary equilibrium contains only a limited amount of the colored form. Few photochromic compounds possess the favorable properties of the 1,2-dithienylperfluorocyclopentene (DTE) skeleton. Such compounds undergo a ring-closing reaction under UV illumination; the closed-ring form returns to the open-ring form when irradiated by green or red light.[2] Both the open and the closed isomers are thermally stable, and the photochromic interconversion between the two states is highly fatigue-resistant.

There have been several attempts to integrate photochromic molecules into organic electronic devices aiming, for example, at data storage. However, the achieved ON/OFF ratios, that is, the ratio of the current density in the ON and OFF states, respectively, did not exceed 100.[3–14] Recently, Zhang et al. reported not only on current but also on electroluminescence (EL) switching of an Alq_3-based OLED (Alq_3 = tris(8-hydroxyquinolino)aluminum). However, these devices required a very large operating voltage. When an additional hole-transporting layer was inserted to reduce the operating voltage, the device could no longer be switched (ON/OFF ca. 2).[14]

Herein, we report on fully solution-processed multiple-layer devices that can be reversibly switched using a photochromic hole-injection layer embedded into the multilayer stack of an OLED. The devices were fabricated by consecutive crosslinking of each layer,[15,16] which allows for systematic optimization of the different layers in terms of high ON/OFF ratio and enables a detailed understanding of the operation principles. We achieve ON/OFF ratios greater than 10^3 for both current density and EL. This result compares favorably with the current state of the art in organic memories.[17]

We synthesized the oxetane-functionalized dithienylethene **1** (XDTE, Figure 1), adapting the methods described in the literature.[18–20] By irradiating the colorless open form (**1o**) with UV light, the deep blue closed form (**1c**) is formed by conrotatory 6π6 electrocyclization. NMR spectroscopy shows that in solution, 95 % **1c** can be achieved (corresponding UV/Vis spectrum in Figure 1). Such high isomerization yield is obtained because the quantum yield of the ring-closing reaction is orders of magnitude larger than the quantum yield of ring opening.[25] **1c** switches back to the open form when illuminated by orange light.

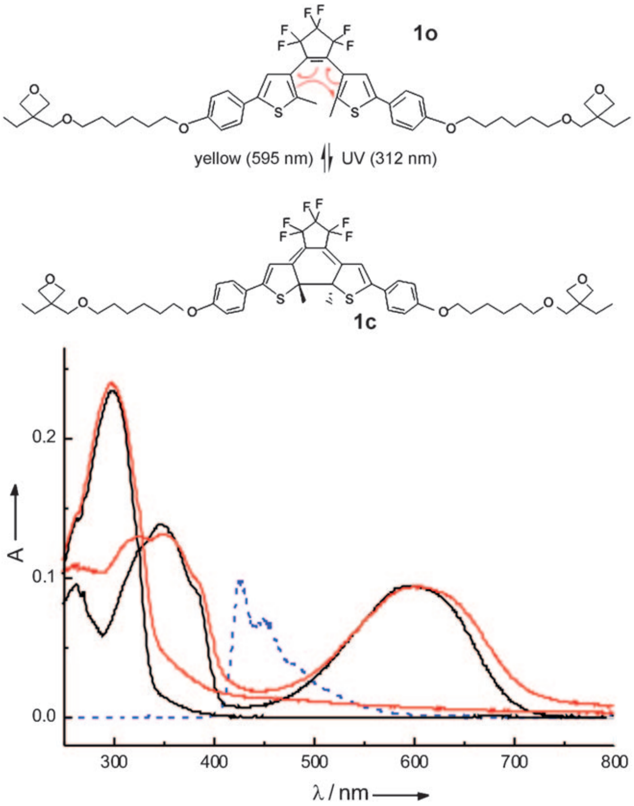

Figure 1. UV/Vis spectra of the colorless open form **1o** and the colored closed form **1c**: 2.5×10^{-6} M solution in CH_2Cl_2 (——), 40 nm crosslinked film on glass (——); electroluminescence spectrum of the photoswitchable device with **B** as emissive layer (-----, arbitrary units).

In the presence of a photoacid, **1** can be crosslinked by photoinitiated cationic ring-opening polymerization (CROP) of the oxetane units. This strategy has been successfully used to fabricate multilayer OLEDs and RGB-pixelated displays from solution.[21–24] In principle, there are two concepts to achieve efficient conversion (open to closed) even inside a solid matrix. Firstly, the matrix should be sufficiently flexible to allow for interconversion between the two conformers of the open-ring state (parallel and antiparallel conformer, where only the latter can undergo ring closure). Secondly, when the DTE is incorporated as the closed-ring isomer into a rigid environment (such as a crosslinked network), the antiparallel conformation can be preserved. This situation prevents conversion of **1o** to the unproductive parallel

---

[*] Dr. P. Zacharias, Dr. M. C. Gather, Dr. A. Köhnen, N. Rehmann, Prof. Dr. K. Meerholz
Department of Chemistry, University of Cologne
Luxemburger Strasse 116, 50939 Cologne (Germany)
Fax: (+49) 221-470-5144
E-mail: klaus.meerholz@uni-koeln.de

Supporting information for this article is available on the WWW under http://dx.doi.org/10.1002/anie.200805969.

conformation and allows efficient ring closure even in rigid matrixes. We choose a flexible molecular structure for our crosslinked photochromic film and switched the XDTE to its closed-ring form prior to film deposition and crosslinking. Figure 1 shows that the UV/Vis spectra of **1** as a crosslinked film and in solution are very similar. Thus, although the polymerization results in an insoluble network, the crosslinked film can be switched to a similar degree as in solution (greater than 90 %).

The isomerization reaction not only affects the optical properties of **1** but also changes its electronic characteristics. Cyclic voltammetry in solution demonstrated that **1c** is reversibly oxidized at $E_{ox}=0.32$ V versus ferrocene/ferrocenium. In contrast, **1o** shows an irreversible oxidation peak at 0.9 V. The HOMO (highest occupied molecular orbital) levels can be estimated by assuming $E_{HOMO}=-5.1\ \mathrm{eV}-E_{ox}$, yielding −5.42 and −6.0 eV for **1c** and **1o**, respectively. It is the difference between the HOMO levels of **1c** and **1o** that we exploit to switch our devices. The emissive material, a blue-emitting polyspirofluorene (**B**), was chosen such that the spectral overlap between its emission and the absorption of the photochromic system was minimized (Figure 1). Thus, in the ON state holes can be injected efficiently via **1c**, while the HOMO level of **1o** results in a large injection barrier (OFF state).

First, we directly incorporated different amounts of **1** into a layer of the electroluminescent polymer that was sandwiched between the two electrodes (device type A, Supporting Information Figure S1). Even the presence of rather small amounts of **1** (0.5 wt %) leads to a strong reduction of the electroluminescent efficiency from about 2 cd A^{-1} (in the absence of **1**) to only 0.1 cd A^{-1} (Supporting Information Figure S2). No significant switching was observed after exposure to UV light. Next, we introduced a layer of **1** between the anode and the emissive layer (device type B, Supporting Information Figure S1). These devices showed EL and could be switched with an ON/OFF ratio of about 5.

Finally, we introduced an additional hole-transport layer between PEDOT:PSS and **1** (device type C, Supporting Information Figure S1; PEDOT = poly(3,4-ethylenedioxythiophene), PSS = poly(styrene-4-sulfonate)). In previous work, we developed a family of crosslinkable hole-transport materials based on triphenylamine dimer (XTPD), which favorably lend themselves to performing the hole injection into the photochromic layer. The most suitable material was selected by systematic device optimization. Seven different XTPDs (**2**–**8**) with HOMO energies ranging from −5.17 to −5.56 eV (Supporting Information Table S1, which includes the chemical structures of the XTPDs) were tested in combination with a 20 nm thick layer of **1**. Among the devices with a single XTPD layer (16 nm), the largest ON/OFF ratios of about 200 were obtained for the case where the HOMO level of the XTPD is close to the PEDOT work function (compounds **2** and **3**). The ON/OFF ratio decreases with decreasing HOMO level, approaching unity for the XTPD with the lowest HOMO energy (compound **8**). Even larger ON/OFF ratios of up to 550 were realized for devices with two different 8 nm thick XTPD layers (**2**/**3** and **2**/**4**; Supporting Information Table S1).

These results can be rationalized as follows: Optimizing the ON/OFF ratio requires minimizing the largest injection barrier for holes (LHIB) in the ON state of the device while at the same time maximizing it in the OFF state. In Figure 2, log(ON/OFF) is plotted as a function of ΔLHIB for all devices studied herein. Clearly, a linear relationship is obtained. The largest ON/OFF ratios correspond to the largest possible ΔLHIB, which is given by the difference between the HOMO levels of **1c** and **1o**, that is, 0.58 eV in our case (•••••, Figure 2).

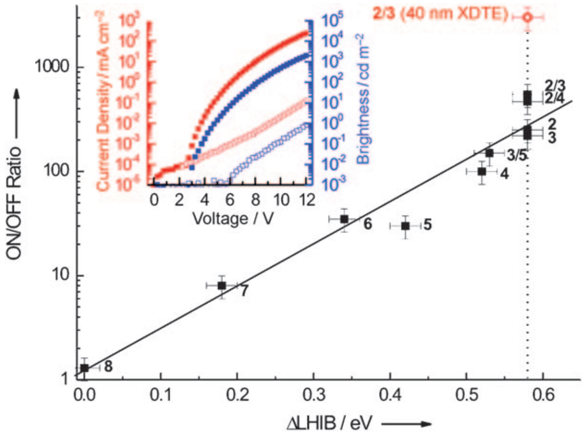

Figure 2. Current ON/OFF ratios as a function of ΔLHIB (LHIB = largest injection barrier for holes). The device structure was PEDOT/XTPD/**1** (20 nm)/**B** (70 nm)/Ba (4 nm)/Al (150 nm), where XTPD was either one layer of XTPD (**2**–**8**, 16 nm) or two layers (8 nm each). The numbers indicate the XTPD used in the particular experiment. Inset: Current density (red) and luminance (blue) characteristics of the optimized device PEDOT (35 nm)/**2** (8 nm)/**3** (8 nm)/**1** (40 nm)/**B** (70 nm)/Ba (4 nm)/Al (150 nm) in the ON (closed symbols) and OFF state (open symbols).

The ON/OFF ratio can be further enhanced by adjusting the thickness of the XDTE layer. In a series of devices with a **2**/**3** XTPD double layer (16 nm total) and increasing XDTE thickness, the ON/OFF ratio increases and shows an optimum at 3000 for a thickness of 40 nm (Supporting Information Figure S3). As for all of our devices, the ON/OFF ratio for the brightness and the current are roughly equal. In the OFF state, the onset of emission is about 6 V. After switching to the ON state by UV irradiation (312 nm), the onset is reduced to 2.7 V (inset Figure 2). By exposure to orange light (590 nm) the device switches back to the OFF state.

The EL efficiency of 0.8 cd A^{-1} ($\lambda_{max}=428$ nm) is almost constant with applied voltage (Supporting Information Figure S4). A reference device in which the photochromic layer was replaced by the XTPD **6** (with a similar HOMO energy of ca. −5.4 eV) reaches 2.1 cd A^{-1} ($\lambda_{max}=456$ nm). Besides poor electron blocking at the interface between **B** and **1** (Supporting Information Figure S4), the lower efficiency of the switchable device is primarily due to its blue-shifted emission (reduced eye sensitivity), which results from a different location of the emission zone.[26] Both the electron blocking and the position of the emission zone were improved by introducing an additional XTPD layer (**7**) between the **1** and **B**.

After optimizing the ON/OFF ratio, we investigated the switching dynamics by simultaneously recording current density and the absorption of the photochromic layer in the complete device using a reflection setup. At a wavelength of 595 nm, the absorption is directly proportional to the concentration of **1c**. For the ring closure induced by UV illumination (312 nm; OFF⇒ON) we observed an exponential increase of the absorption (Figure 3 A). The rate constant was $k_{\text{closure}} = 20\ \text{J}^{-1}\,\text{cm}^2$. For the ring-opening reaction induced by orange illumination (590 nm; ON⇒OFF) the rate constant was $k_{\text{opening}} = 3.4\ \text{J}^{-1}\,\text{cm}^2$ (Figure 3 B).

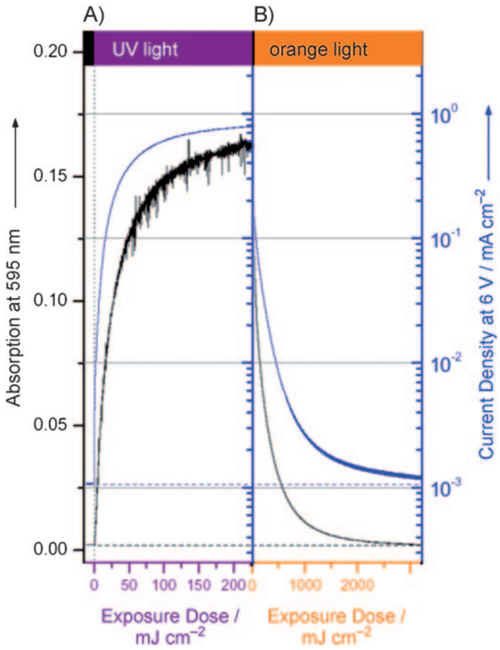

Figure 3. Switching dynamics of the optimized device PEDOT (35 nm)/**2** (8 nm)/**3** (8 nm)/**1** (40 nm)/**B** (70 nm)/Ba (4 nm)/Al (150 nm), simultaneously measuring the absorption of the photochromic layer (——, left axis) and the current density (——, right axis). The applied voltage was 6 V. A) Under UV irradiation (312 nm; OFF⇒ON). B) Under irradiation with orange light (590 nm; ON⇒OFF).

Further, we tested the fatigue resistance towards repeated switching of the XDTE layer inside the device. We obtained a cyclability of $Z_{80} \approx 190$, similar to what was reported for the 5-phenyl analogue in hexane.[2] This result indicates that the high fatigue resistance of the photochromic material is preserved in the photoswitchable device.

As an application of the photochromic devices, we propose to individualize the active area of OLEDs, for example for signage (Figure 4). Starting in the all-ON state (Figure 4 B), irradiation with orange light through a shadow mask (Figure 4 D) resulted in writing an information-containing state (Figure 4 E) that was read out using a conventional CCD camera. Subsequent homogenous irradiation with orange light erased the information and gave the all-OFF state (Figure 4 C). The inverted information-containing state (Figure 4 F) was obtained after exposure through the mask by UV light.

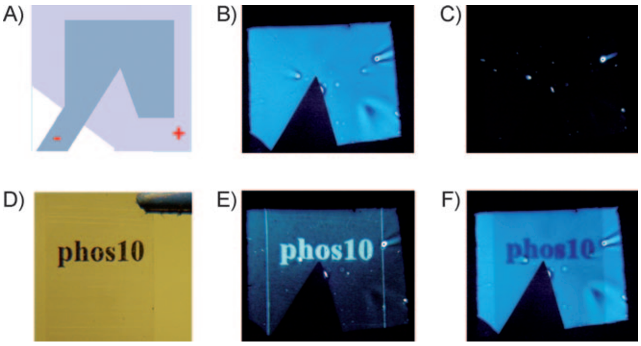

Figure 4. Individualization of the emissive area. A) Layout of the device (light gray: indium tin oxide (ITO), dark gray: metal electrode). The pronged shape of the active area allows for easy recognition. B) Photograph of the photoswitchable OLED in the all-ON state after homogenous UV irradiation. C) Photograph in the all-OFF state after homogenous illumination with orange light. D) Shadow mask (laser printer sheet). E,F) Individualized states after mask exposure with orange and UV light starting from the all-ON (E) or all-OFF state (F). The bright spots seen in (B), (C), (E), and (F) are due to processing imperfections (pinholes) in the photochromic layer.

In conclusion, we demonstrated an OLED that can be manipulated by means of external irradiation. The cross-linking capability of the XDTE allowed for systematic device engineering in a similar way as commonly done in state-of-the-art small-molecule devices fabricated by vapor deposition. Optimized devices contained up to six solution-processed layers, each with a dedicated function. Unlike many cases in the literature, the storage principle in our device is well-understood. The optimized device showed ON/OFF ratios of about 3000. The information can be programmed and erased multiple times and can also be stored without noticeable change over ten months (the time we studied to date).

Experimental Section

Synthesis of **1**: *n*-Butyllithium (1.65 M solution in hexane, 1.14 mL, 1.88 mmol, 2.54 equiv) was added at −78 °C to the corresponding 3-bromothiophene (760 mg, 1.63 mmol, 2.2 equiv) in THF (8 mL). The mixture was stirred for 45 min before octafluorocyclopentene (157 mg, 0.74 mmol) was added. The reaction mixture was stirred in the dark at −78 °C for 2 h, then allowed to warm up to room temperature while stirring for another 2.5 h. The mixture was diluted 1:1 with *tert*-butyl methyl ether; the ether phase was washed with water, dried, and concentrated. The resulting oil was dissolved in acetonitrile (2 mL) and purified by reversed-phase MPLC (MeOH on RP18-SiO_2, 20 mL min^{-1}), yielding **1o** (370 mg, 53 %).

Cyclic voltammograms were recorded on a potentiostat/galvanostat (EG + G Instruments M283) in CH_2Cl_2 solution (10^{-3} M) containing NBu_4PF_6 (10^{-1} M) as electrolyte and calibrated versus ferrocene/ferrocenium.

Devices were fabricated on thoroughly cleaned and O_3-treated glass–ITO substrates. A layer of PEDOT:PSS (35 nm, Baytron P AI4083) was spin-coated onto the substrates and dried for 80 s at 110 °C. The substrates were transferred to a N_2 glove box and the XTPD layers were spin-coated from toluene solutions (2.5 g L^{-1}) containing 4.0 mol % 4-octyloxydiphenyliodonium hexafluorantimonate (OPPI) as photoinitiator. The films were irradiated with UV light (360 nm, 10 s), cured at 110°C for 100 s, and rinsed with THF. The dithienylethene **1** (7 $\mathrm{g\,L^{-1}}$ in toluene, 5.6 mol% OPPI) was switched to the closed-ring state by UV exposure and spin-coated on top of the XTPD layer, irradiated with UV light (312 nm, 60 s), cured at 110°C for 150 s, and rinsed with THF. The emissive polymer **B** (8 $\mathrm{g\,L^{-1}}$ in toluene) was spin-coated on top. Subsequently, the cathode (4 nm Ba, 150 nm Al) was deposited by thermal evaporation at a base pressure of 10^{-9} bar. The samples were encapsulated for extensive characterization outside the glovebox. Current–voltage–luminescence characteristics were measured with a Keithley 2400 source meter and a calibrated photodiode.

Received: December 8, 2008

Keywords: charge carrier injection · organic light-emitting devices · organic memory · photochromism · solution processing

---

[1] H. Bouas-Laurent, H. Dürr, *Pure Appl. Chem.* **2001**, *73*, 639.

[2] M. Irie, *Chem. Rev.* **2000**, *100*, 1685.

[3] M. Yokoyama, T. Honma, *Denshi Shashin Gakkaishi* **1997**, *36*, 5.

[4] M. Yokoyama, T. Honma in IS&T's 13th International Conference on Digital Printing Technologies **1997**, p. 225.

[5] T. Kawai, Y. Nakashima, M. Irie, *Adv. Mater.* **2005**, *17*, 309.

[6] P. Andersson, N. D. Robinson, M. Berggren, *Adv. Mater.* **2005**, *17*, 1798.

[7] P. Toman, S. Nespurek, M. Weiter, M. Vala, J. Sworakowski, W. Bartkowiak, M. Mensik, *Nonlinear Opt.* **2007**, *37*, 87.

[8] M. Weiter, M. Vala, O. Zmeskal, S. Nespurek, P. Toman, *Macromol. Symp.* **2007**, *247*, 318.

[9] X. F. Guo, D. Zhang, Y. Gui, M. X. Wax, J. C. Li, Y. Q. Liu, D. B. Zhu, *Adv. Mater.* **2004**, *16*, 636.

[10] T. Tsujioka, N. Iefuji, A. Jiapaer, M. Irie, S. Nakamura, *Appl. Phys. Lett.* **2006**, *89*, 222102.

[11] T. Tsujioka, H. Kondo, *Appl. Phys. Lett.* **2003**, *83*, 937.

[12] T. Tsujioka, K. Masuda, *Appl. Phys. Lett.* **2003**, *83*, 4978.

[13] T. Tsujioka, M. Shimizu, E. Ishihara, *Appl. Phys. Lett.* **2005**, *87*, 213506.

[14] Z. Zhang, X. D. Liu, Z. Y. Li, Z. I. Chen, F. Q. Zhao, F. I. Zhang, C. H. Tung, *Adv. Funct. Mater.* **2008**, *18*, 302.

[15] K. Meerholz, C. D. Mueller, O. Nuyken in *Organic Light-Emitting Devices* (Ed.: U. Scherf), Wiley-VCH, Weinheim, **2005**, p. 293.

[16] D. C. Müller, T. Braig, H. G. Nothofer, M. Arnoldi, M. Gross, U. Scherf, O. Nuyken, K. Meerholz, *ChemPhysChem* **2000**, *1*, 207.

[17] J. C. Scott, L. D. Bozano, *Adv. Mater.* **2007**, *19*, 1452.

[18] M. G. Reinecke, H. W. Adickes, C. Pyun, *J. Org. Chem.* **1971**, *36*, 2690.

[19] S. O. Lawesson, *Ark. Kemi* **1957**, *11*, 387.

[20] S. H. Kawai, S. L. Gilat, R. Ponsinet, J. M. Lehn, *Chem. Eur. J.* **1995**, *1*, 285.

[21] C. D. Müller, A. Falcou, N. Reckefuss, M. Rojahn, V. Wiederhirn, P. Rudati, H. Frohne, O. Nuyken, H. Becker, K. Meerholz, *Nature* **2003**, *421*, 829.

[22] M. C. Gather, A. Köhnen, A. Falcou, H. Becker, K. Meerholz, *Adv. Funct. Mater.* **2007**, *17*, 191.

[23] P. Zacharias, M. C. Gather, M. Rojahn, O. Nuyken, K. Meerholz, *Angew. Chem.* **2007**, *119*, 4467; *Angew. Chem. Int. Ed.* **2007**, *46*, 4388.

[24] N. Rehmann, C. Ulbricht, A. Köhnen, P. Zacharias, M. C. Gather, D. Hertel, U. S. Schubert, K. Meerholz, *Adv. Mater.* **2008**, *20*, 129.

[25] M. Irie, K. Sakemura, M. Okinaka, K. Uchida, *J. Org. Chem.* **1995**, *60*, 8305.

[26] M. C. Gather, R. Alle, H. Becker, K. Meerholz, *Adv. Mater.* **2007**, *19*, 4460.